Efficient Antenna Systems: A New Computer Program for the Design and Analysis of High-Performance Conical Feedhorns

P. D. Potter
Communications Elements Research Section

It is well known that paraboloidal antenna aperture efficiency is enhanced by providing aperture illumination which approaches uniformity in amplitude, phase, and polarization. For dual-reflector antenna systems, such as those used in the DSN, a high degree of uniformity is possible by use of specially shaped reflector surfaces (Ref. 1). As a long-range solution to the problem of achieving high aperture efficiency, this approach is attractive because it is inherently broadband and requires only a simple feedhorn of the type presently being utilized in the DSN. An alternate approach for achieving high aperture efficiency (suggested by D. Bathker of the Communications Elements Research Section) involves use of the existing antenna reflecting surfaces together with a more complex multimode feedhorn. This approach is attractive from an implementation standpoint. Preliminary experimental results (obtained by R. Thomas of the Communications Elements Research Section) are promising. The multimode technique does, however, suffer from bandwidth difficulties, at least with presently known mode-generation techniques. To assist and guide the multimode feedhorn experimental effort, a new computer program has been developed which computes horn radiation patterns and bandwidth properties as a function of horn geometry. This article describes the analytical technique utilized and agreement with existing experimental data.

I. Introduction

For the case of conical horns with modest or small flare angles, the amplitude patterns may be calculated to good accuracy by expanding the aperture fields in cylindrical waveguide modes and utilizing the radiation pattern formulas given by Silver (Ref. 2). An early but definitive work on the effect of neglecting the horn flare angle by Ludwig (Ref. 3) showed that the propagation characteristics of conical waveguide modes differ from those of cylindrical waveguide modes in a simple and predictable way. In a detailed analysis of the differences in aperture illumination functions between cylindrical and conical modes, Narasimhan and Rao (Ref. 4) demonstrate that, for semi-flare angles up to 20 deg, the fields on a spherical cap in the horn aperture are very well approximated by the standard cylindrical (Bessel function) fields.

The first good conical feedhorn to be developed was the dual-mode horn reported by Potter (Ref. 5). This horn has many desirable performance features, together with a convenient physical configuration, but suffers from a bandwidth problem. The dual-mode horn concept was extended by Ludwig (Ref. 6) to the case of many modes. Ludwig used cylindrical waveguide functions and showed good experimental results for a four-mode horn. Later, Minnet and Thomas (Ref. 7) reported a new technique for achieving the same performance as the dual-mode horn (Ref. 5) but over a large bandwidth. This method consists of utilizing a high-impedance wall in the horn, physically realized by circumferential grooves approximately one-quarter wavelength deep. The two modes in such a horn (TE_{11} and TM_{11}) propagate with the same velocity and are both necessary in a certain phase and amplitude relationship to satisfy the horn wall boundary conditions. The two modes are therefore called a single hybrid mode, designated the HE_{11} mode. A horn of this type is presently the standard design for the DSN 64-m-diameter antennas (Ref. 8).

B. Mac A. Thomas later extended his hybrid-mode horn analysis to the case of multiple hybrid modes (Ref. 9). In order to get closed-form solutions for the modal radiation patterns, Thomas assumed a planar aperture with cylindrical hybrid modes. A definitive review of hybrid-mode propagation and aperture radiation for both cylindrical and conical configurations has been published by Clarricoats and Saha (Refs. 10 and 11).

Clarricoats et al. (Ref. 12) developed a spherical wave technique for computing hybrid-mode horn radiation patterns and showed good agreement with experimental data. Professor Clarricoats was kind enough to send a copy of the computer program developed by his group for performing these radiation pattern calculations. Unfortunately, his program (written in ALGOL) was not easily adaptable for use with the JPL Scientific Computing Facility (SCF). Additionally, certain extra features were desired in the program. For these reasons, a new program was written in FORTRAN IV for use on the SCF Univac 1108 computer. This program utilizes Clarricoats' spherical wave technique (Ref. 12) and his cylindrical hybrid-mode equations (Ref. 10) but uses a spherical cap aperture with the field approximation of Ref. 4. This procedure produces very accurate results for small flare-angle horns such as those employed in DSN antennas. The new computer program has been checked out and results have been compared with experimental data. The program is described in the next section.

II. Computer Program Description

Figure 1 shows the selected horn geometry. The phasing section may have zero length as a special case, or may be utilized to phase a pair of hybrid modes for proper relationship. The computer program, HYBRID-HORN, assumes that the amplitude of the hybrid modes in the aperture is known and has an input for adjustment of mode amplitudes; in actual practice, the mode amplitudes are controlled by the mode-generator geometry. The phases of the hybrid modes at the input of the phasing section (mode generator) are also input. The resulting phases at the aperture are computed by numerical integration of the propagation constants in the phasing section and flare. The propagation constants in the flare are calculated using the cylindrical-guide-arc length technique developed by Ludwig (Ref. 3). The only other program inputs are the horn physical geometry and various output options. A typical case (one geometry at one frequency) takes about 20 s of SCF Univac 1108 execution time.

The program presently assumes unity ($m = 1$) azimuthal field variation, although it could easily be upgraded for modes with arbitrary azimuthal variation. The $m = 1$ variation is that which is normally desired in an antenna feed. The field equations in the horn plane are given by (Ref. 10):

$$\mathbf{E}_{rn} = (E_n)\,[J_1(x)]\sin\phi\mathbf{a}_r \tag{1a}$$

$$\mathbf{H}_{rn} = -\left(\frac{E_n}{Z_0}\right)(\mathrm{BAL}_n)\,[J_1(x)]\cos\phi\mathbf{a}_r \tag{1b}$$

$$\mathbf{E}_{\theta n} = -j(E_n)\left(\frac{k}{K_n}\right)\left[\frac{J_1(x)}{x}\right] \times [\bar{\beta}_n \cdot F_m(x) + \mathrm{BAL}_n]\sin\phi\mathbf{a}_\theta \tag{1c}$$

$$\mathbf{E}_{\phi n} = -j(E_n)\left(\frac{k}{K_n}\right)\left[\frac{J_1(x)}{x}\right] \times [\bar{\beta}_n + F_m(x) \cdot \mathrm{BAL}_n]\cos\phi\mathbf{a}_\phi \tag{1d}$$

$$\mathbf{H}_{\theta n} = +j\left(\frac{E_n}{Z_0}\right)\left(\frac{k}{K_n}\right)\left[\frac{J_1(x)}{x}\right] \times [\bar{\beta}_n \cdot \mathrm{BAL}_n \cdot F_m(x) + 1]\cos\phi\mathbf{a}_\theta \tag{1e}$$

$$\mathbf{H}_{\phi n} = -j\left(\frac{E_n}{Z_0}\right)\left(\frac{k}{K_n}\right)\left[\frac{J_1(x)}{x}\right] \times [\bar{\beta}_n \cdot \mathrm{BAL}_n + F_m(x)]\sin\phi\mathbf{a}_\phi \tag{1f}$$

where

$$F_m(x) \equiv x\left[\frac{J_1'(x)}{J_1(x)}\right]$$

J_1 = Bessel function of the first kind and order 1

J_1' = derivative of J_1 with respect to the argument

k = free-space propagation constant

$x = K_n r$

Z_0 = free-space characteristic impedance

$$F_m(x_1) - \frac{\bar{\beta}_n^2}{F_m(x_1)} = \left(\frac{K_n}{k}\right)^2 S_m(x_1', x_0') \tag{2}$$

$$F_m(x_1) = x_1\left[\frac{J_1'(x_1)}{J_1(x_1)}\right]$$

$x_1 = Kr_1$

$$\bar{\beta}_n^2 \equiv 1 - \left(\frac{K_n}{k}\right)^2$$

$$S_m(x_1', x_0') \equiv x_1'\left[\frac{J_1'(x_1')\cdot Y_1(x_0') - J_1(x_0')\cdot Y_1'(x_1')}{J_1(x_1')\cdot Y_1(x_0') - J_1(x_0')\cdot Y_1(x_1')}\right]$$

Y_1 = Bessel function of the second kind and order 1

Y_1' = derivative of Y_1 with respect to the argument

$x_1' = kr_1$

$x_0' = K(r_1 + \text{GROOVE})$

GROOVE = groove depth

$$\text{BAL}_n = -\frac{\bar{\beta}_n}{F_m(x_1)}$$

The normalized longitudinal propagation constant $\bar{\beta}$ is determined by numerical solution of Eq. (2). The wall reactance, ZGROOV, is given by

$$\text{ZGROOV} = -\frac{(Z_0)x_1'}{S_m(x_1', x_0')} \tag{3}$$

At the frequency of operation for which BAL_n is ± 1, the hybrid mode is said to be *balanced*. Modes for which the BAL_n are positive quantities are normally desired and are designated HE_{1n}. At the balance frequency, the HE_{1n} modes exhibit almost perfect symmetry between E- and H-planes. Modes for which the BAL_n are negative are designated EH_{1n} modes and are normally undesirable since they are grossly unsymmetrical between E- and H-planes.

An interesting and important special case of Eqs. (1a)–(1f) is that for which the groove depth approaches zero, i.e., the horn becomes a standard smooth-wall horn. For this case, BAL_n approaches a positive zero (HE_{1n} modes) or a negative infinity (EH_{1n} modes). Examination of the equations for smooth-wall cylindrical waveguides (Ref. 2) shows that Eqs. (1a)–(1f) become the smooth-wall equations, with HE_{1n} modes becoming TM_{1n} modes and EH_{1n} modes becoming TE_{1n} modes. The case of TE_{11} and TM_{11} is of particular interest since it corresponds to the dual-mode conical horn (Ref. 5), for which good experimental data are available and which is still being used for special applications such as gain standards. The computer program HYBRIDHORN has an internal switch so that it will handle the case of zero groove depth (smooth-wall horn).

III. Comparison with Experimental Data

Figure 2 shows a comparison of HYBRIDHORN computed data (TE_{11} and TM_{11} modes only) for the smooth-wall JPL/NBS Standard Gain Horn (Ref. 13), which is a scale model of the original dual-mode horn design (Ref. 5). The H-plane agreement is almost perfect. The minor discrepancies in E-plane are not presently understood. An attempt was made to improve agreement with experimental data by addition of radiation from currents at the edge of the horn aperture. Significant improvement was not obtained, however. One possibility for the E-plane discrepancies not yet investigated is the presence of significant amounts of modes other than TE_{11} and TM_{11} — the TE_{12} in particular. Although the horn design (Ref. 5) is such that higher-order modes are severely attenuated, the exact degrees of attenuation and the generated amplitudes have not been calculated or measured.

Figure 3 shows a comparison of HYBRIDHORN computed and measured data for the DSIF single hybrid-mode corrugated horn (Ref. 8). These recently obtained measured patterns were taken by R. Thomas and O. Hester of the Communications Elements Research Section, using

the JPL Mesa Antenna Range Facility, with the same basic setup described in Ref. 13. The excellent agreement between computed and measured patterns demonstrates the high quality of the experimental data and the implied accuracy of the HYBRIDHORN computer program.

Figure 4 shows computed and measured amplitude patterns (phase data were not available) for an experimental dual hybrid-mode horn.*

Section IV briefly discusses a novel use of the DSIF standard corrugated feedhorn design, in conjunction with the HYBRIDHORN program.

IV. Possible Use of the DSIF Corrugated Feedhorn Design as a Gain Standard

The HYBRIDHORN computed pattern shown in Fig. 2 was numerically integrated; the computed directivity is 21.990 dB. Despite the minor pattern discrepancies, this number compares favorably with the JPL/NBS horn calibration directivity of 22.04 $\pm$0.10 dB, 3σ, quoted in Ref. 13. The computed directivity of the single hybrid-mode horn pattern shown in Fig. 4 is 22.370 dB (at 8.448 GHz). Because this horn is a single-mode horn, there is no question of whether the HYBRIDHORN program has the correct inputs; thus the confidence level in the 22.370-dB number is high. As a gain standard, the corrugated horn has a number of attractive features relative to the JPL/NBS horn, including lower dissipative loss, lower E-plane aperture edge illumination (hence less exterior currents), broad bandwidth, and more accurately calculable performance. These features bear further examination.

*The computed data are for HE_{11} and HE_{12} modes only. The possibility of additional modes in the experimental data exists.

Acknowledgement

It is a pleasure to acknowledge many helpful discussions on this project with R. Thomas, A. C. Ludwig, and P. W. Cramer, all of the Communications Elements Research Section.

References

1. Potter, P. D., "Antenna Study: Performance Enhancement," in *The Deep Space Network Progress Report*, Technical Report 32-1526, Vol. X, pp. 129–134, Jet Propulsion Laboratory, Pasadena, Calif., Aug. 15, 1972.

2. Silver, S., *Microwave Antenna Theory and Design*, Chapter 10, McGraw-Hill Book Co., Inc., New York, 1949.

3. Ludwig, A., "Antennas for Space Communications: Antenna Feed Research," in *Supporting Research and Advanced Development*, Space Programs Summary 37-22, Vol. IV, pp. 184–189, Jet Propulsion Laboratory, Pasadena, Calif., Aug. 31, 1963.

4. Narasimhan, M. S., and Rao, B. V., "Hybrid Modes in Corrugated Conical Horns," *Electronic Letters*, Vol. 6, No. 2, Jan. 22, 1970, pp. 32–34.

5. Potter, P. D., "A New Horn Antenna with Suppressed Sidelobes and Equal Beamwidths," *Microwave J.*, June 1963.

6. Ludwig, A. C., "Radiation Pattern Synthesis for Circular Aperture Horn Antennas," *IEEE Trans. on Antennas and Propagation*, Vol. AP-14, No. 4, July 1966, pp. 434–440.

7. Minnett, H. C., and Thomas, B. Mac A., "A Method of Synthesizing Radiation Patterns with Axial Symmetry," *IEEE Trans. on Antennas and Propagation*, Vol. AP-14, 1966, pp. 654–656.

8. Brunstein, S. A., "A New Wideband Feed Horn With Equal E- and H-Plane Beamwidths and Suppressed Sidelobes," in *The Deep Space Network*, Space Programs Summary 37-58, Vol. II, pp. 61–64, Jet Propulsion Laboratory, Pasadena, Calif., July 31, 1969.

9. Thomas, B. Mac A., "Theoretical Performance of Prime-Focus Paraboloids Using Cylindrical Hybrid-Mode Feeds," *Proc. IEE (British)*, Vol. 118, No. 11, Nov. 1971.

10. Clarricoats, P. J. B., and Saha, P. K., "Propagation and Radiation Behavior of Corrugated Feeds – Part 1. Corrugated Waveguide Feed," *Proc. IEE (British)*, Vol. 118, No. 9, Sept. 1971, pp. 1167–1176.

11. Clarricoats, P. J. B., and Saha, P. K., "Propagation and Radiation Behavior of Corrugated Feeds – Part 2. Corrugated-Conical-Horn Feed," *Proc. IEE (British)*, Vol. 118, No. 9, Sept. 1971, pp. 1177–1186.

12. Clarricoats, P. J. B., et al., "Near-Field Radiation Characteristics of Corrugated Horns," *Electronic Letters*, Vol. 7, No. 16.

13. Ludwig, A., et al., *Gain Calibration of a Horn Antenna Using Pattern Integration*, Technical Report 32-1572, Jet Propulsion Laboratory, Pasadena, Calif., Oct. 1, 1972.

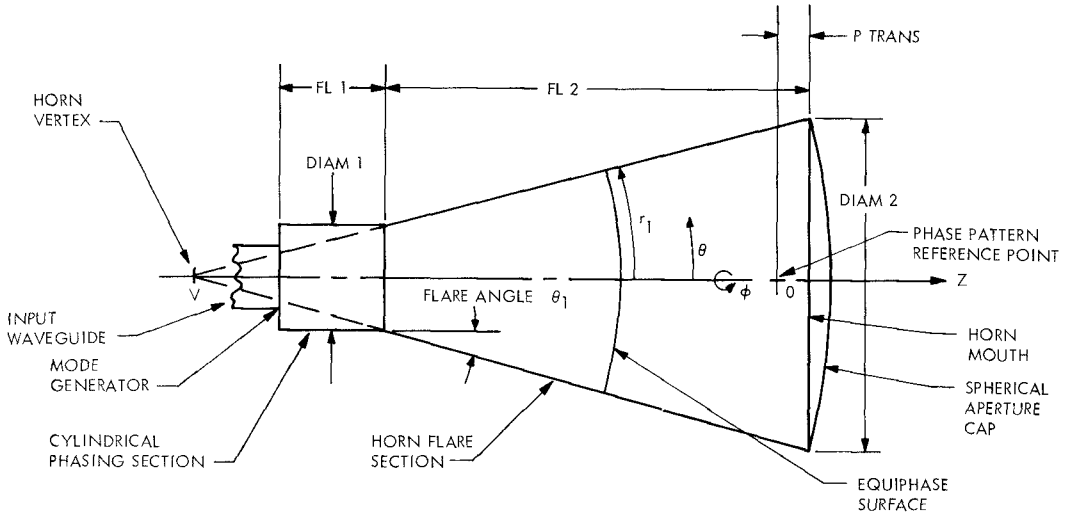

Fig. 1. Horn geometry

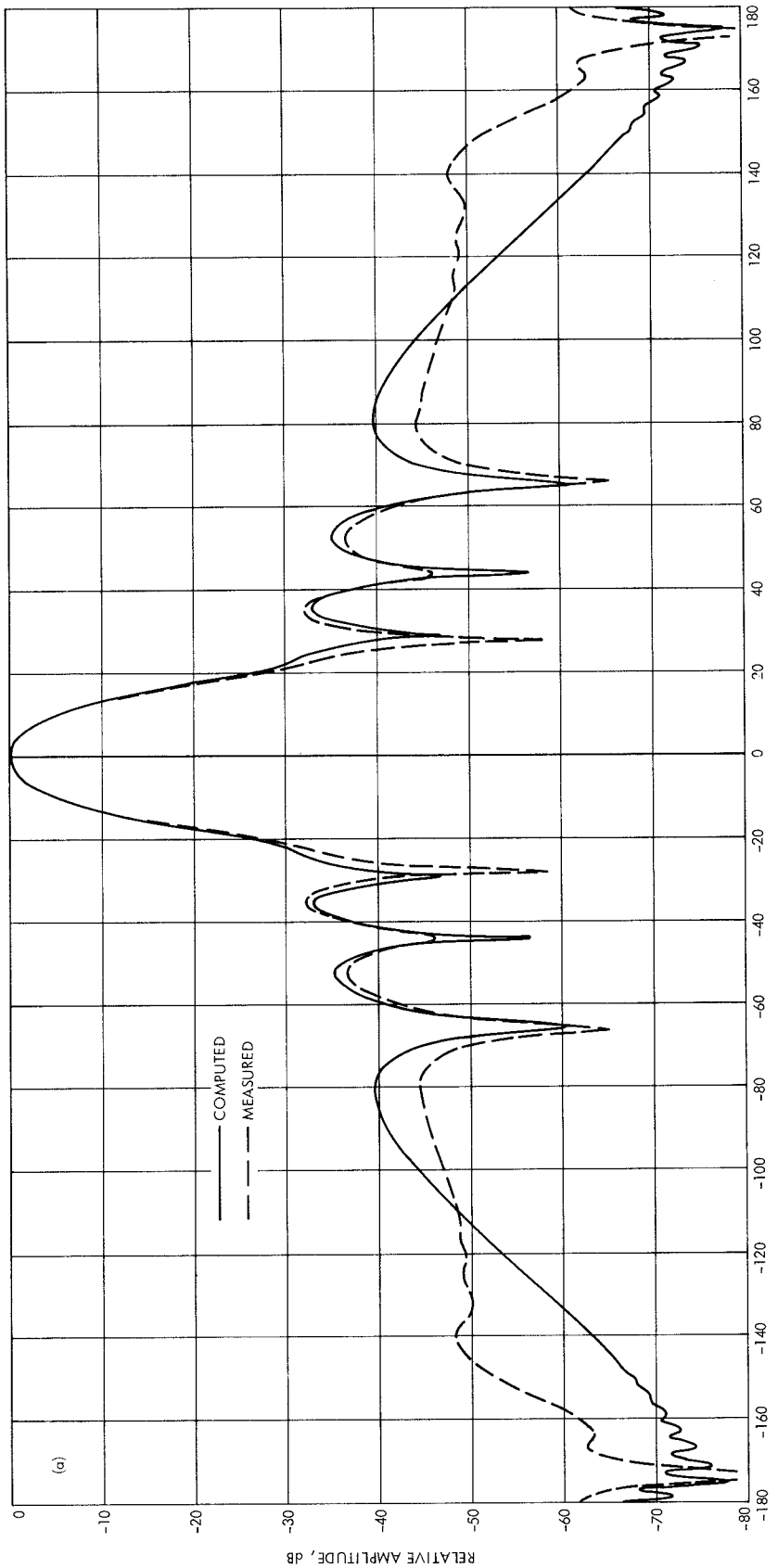

Fig. 2. Computed and measured patterns about phase center, NBS standard gain horn: (a) E-plane amplitude, (b) E-plane phase, (c) H-plane amplitude, (d) H-plane phase

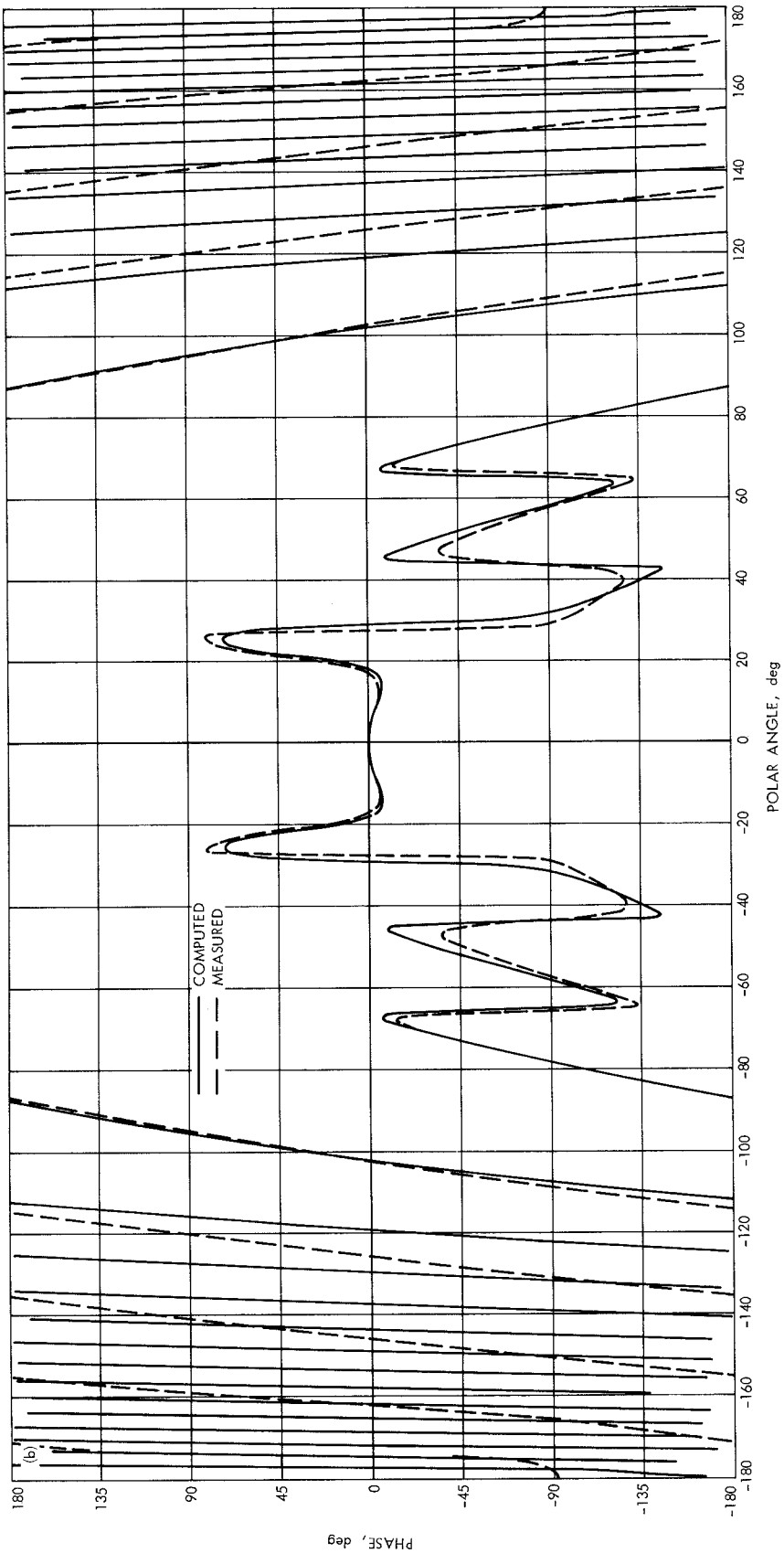
(b)
COMPUTED
MEASURED
PHASE, deg
180
135
90
45
0
-45
-90
-135
-180
POLAR ANGLE, deg
180
160
140
120
100
80
60
40
20
0
-20
-40
-60
-80
-100
-120
-140
-160
-180

Fig. 2 (contd)

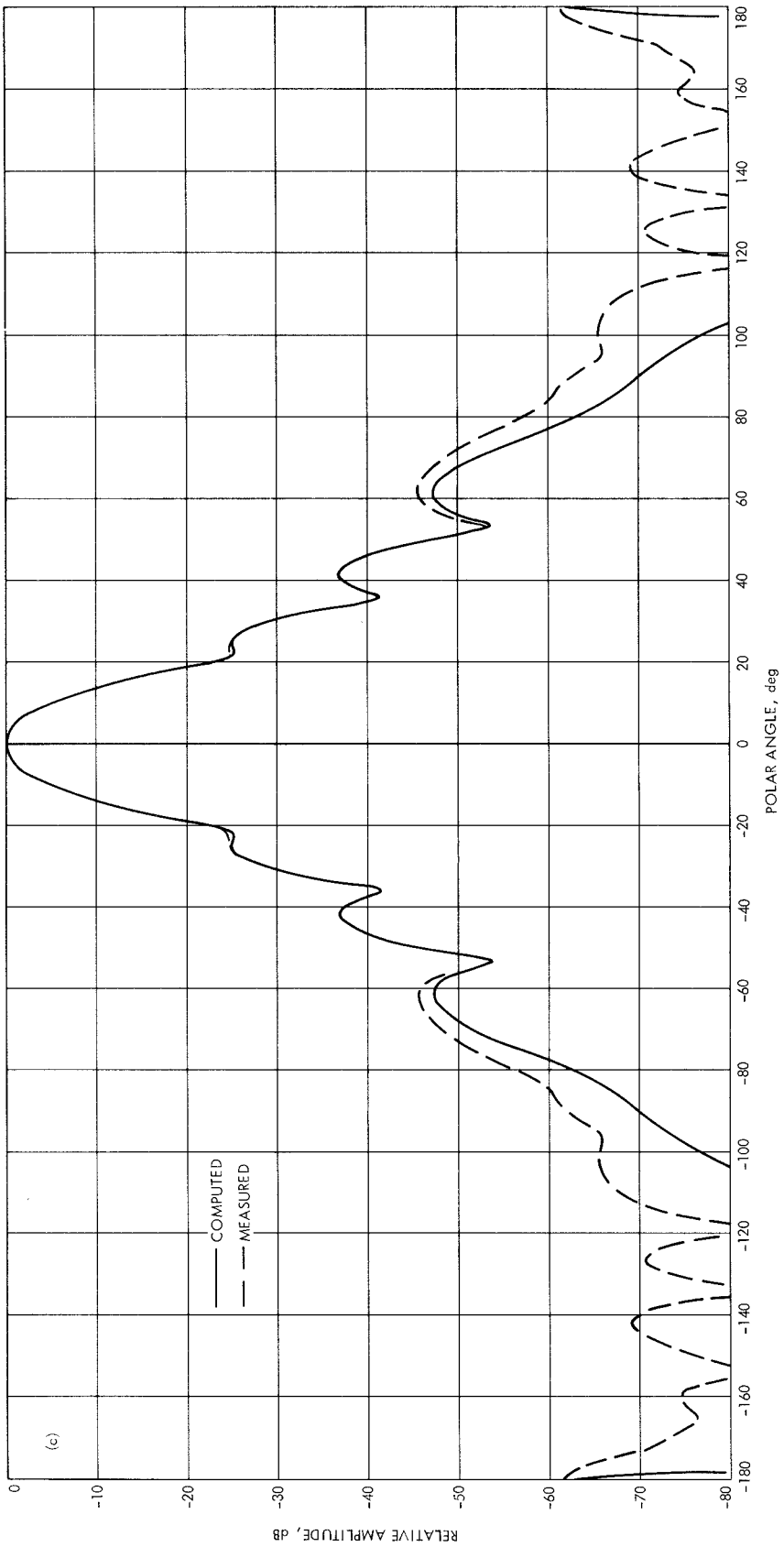
(c)
COMPUTED
MEASURED
RELATIVE AMPLITUDE, dB
0
-10
-20
-30
-40
-50
-60
-70
-80
POLAR ANGLE, deg
180
160
140
120
100
80
60
40
20
0
-20
-40
-60
-80
-100
-120
-140
-160
-180

Fig. 2 (contd)

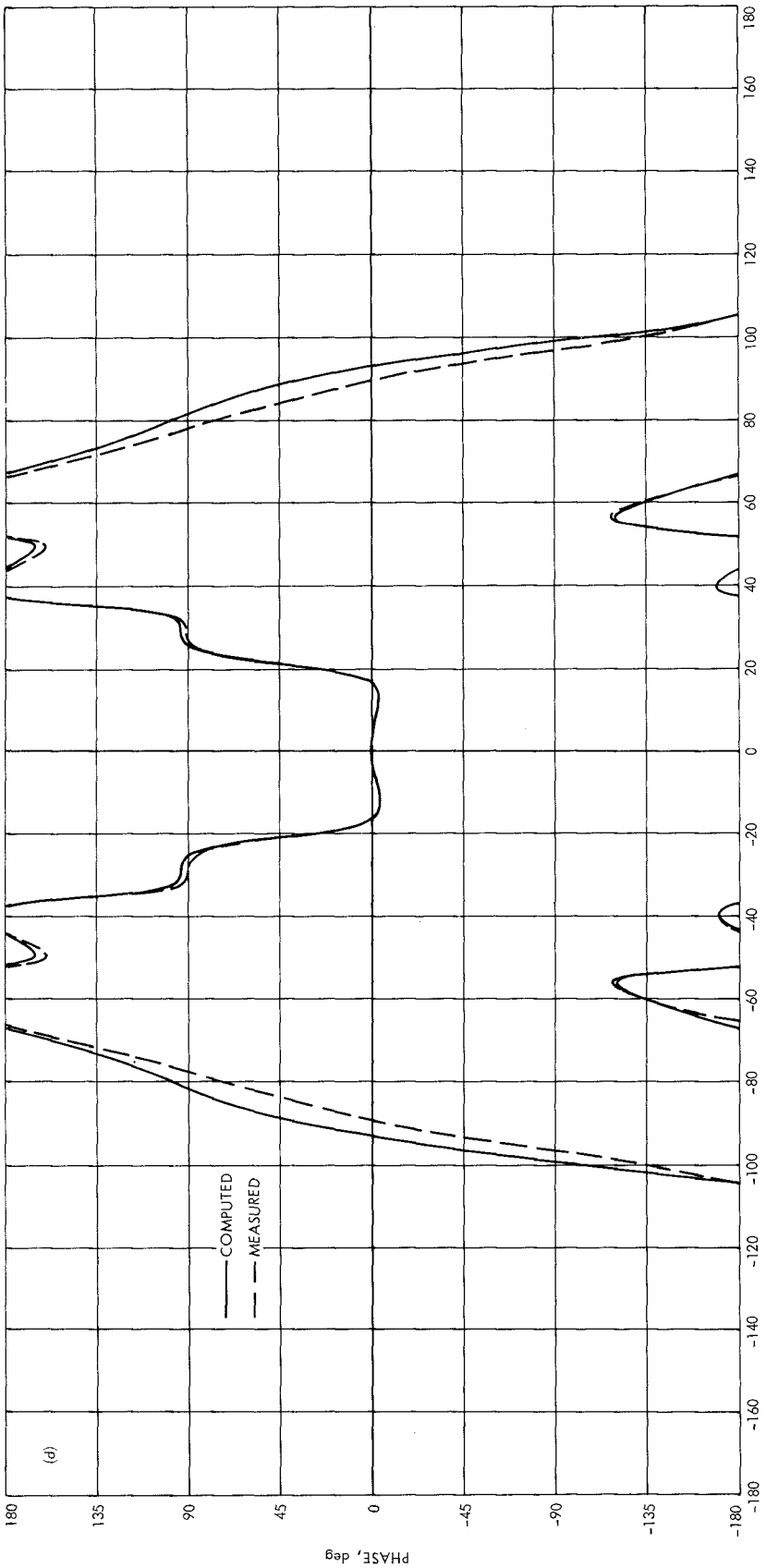
(d)
COMPUTED
MEASURED
PHASE, deg
180
135
90
45
0
-45
-90
-135
-180
POLAR ANGLE, deg
180
160
140
120
100
80
60
40
20
0
-20
-40
-60
-80
-100
-120
-140
-160
-180

Fig. 2 (contd)

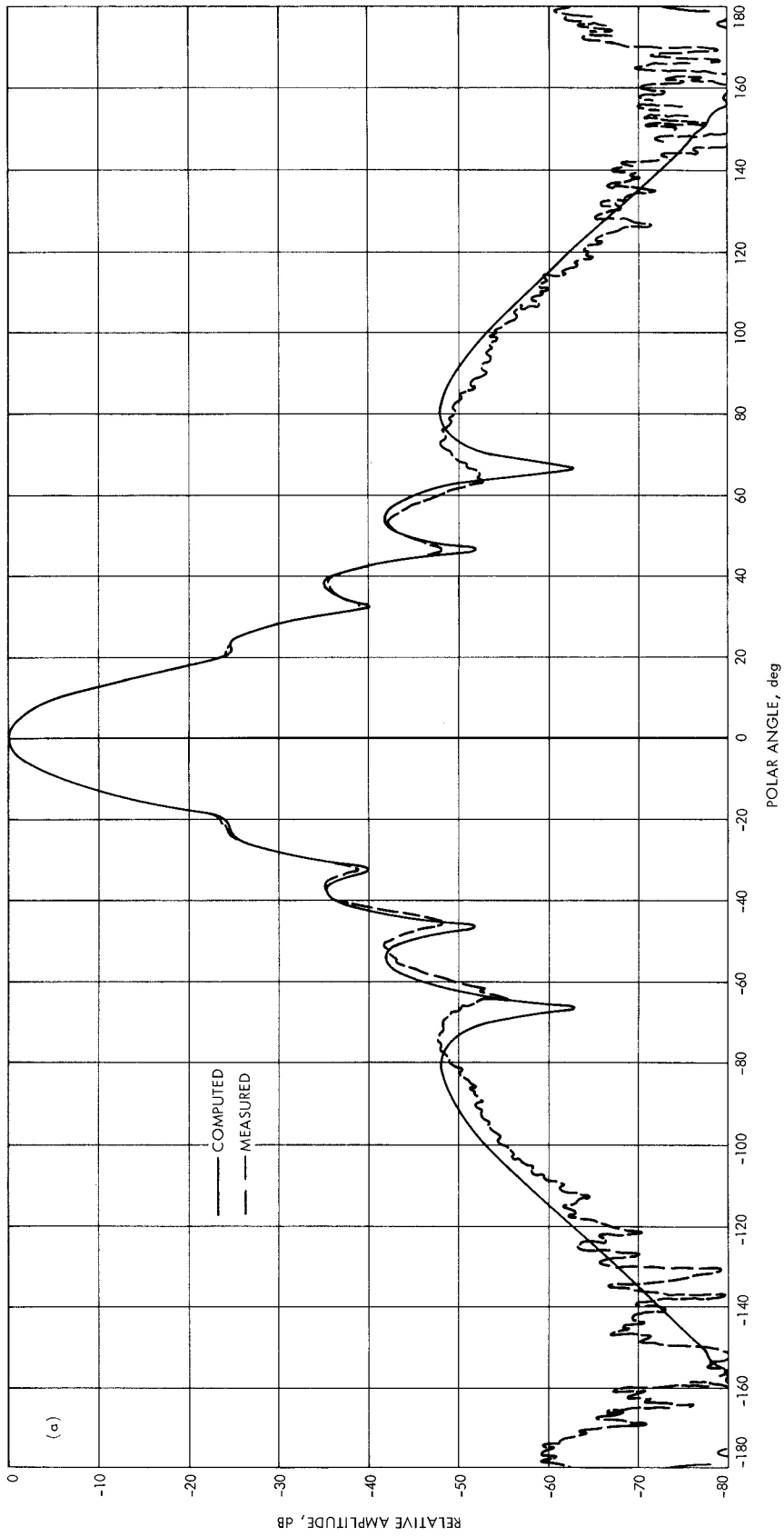

Fig. 3. Computed and measured patterns about phase center, standard DSIF single hybrid-mode horn: (a) E-plane amplitude, (b) E-plane phase, (c) H-plane amplitude, (d) H-plane phase

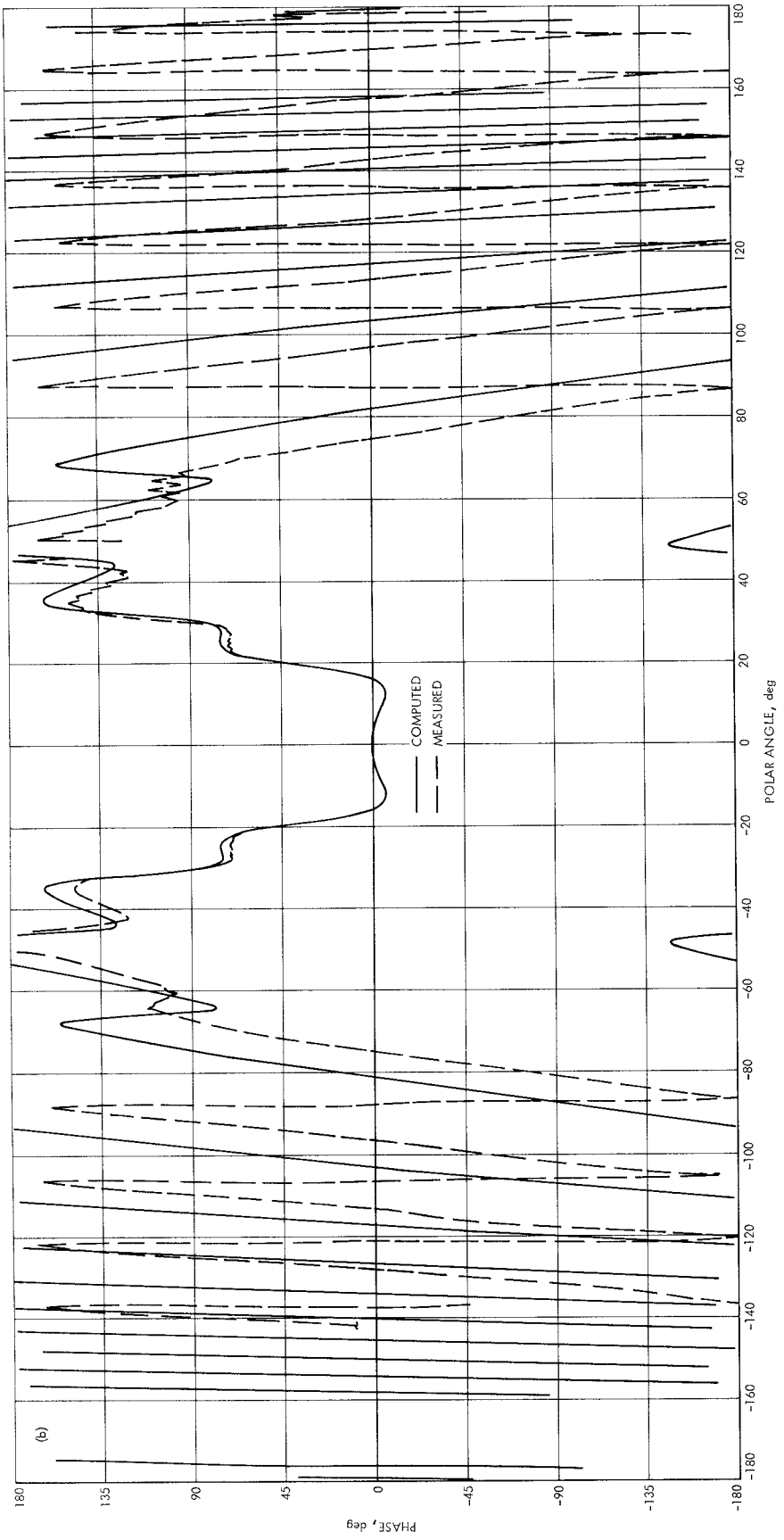
(b)
COMPUTED
MEASURED
PHASE, deg
POLAR ANGLE, deg
180
135
90
45
0
-45
-90
-135
-180
180
160
140
120
100
80
60
40
20
0
-20
-40
-60
-80
-100
-120
-140
-160
-180

Fig. 3 (contd)

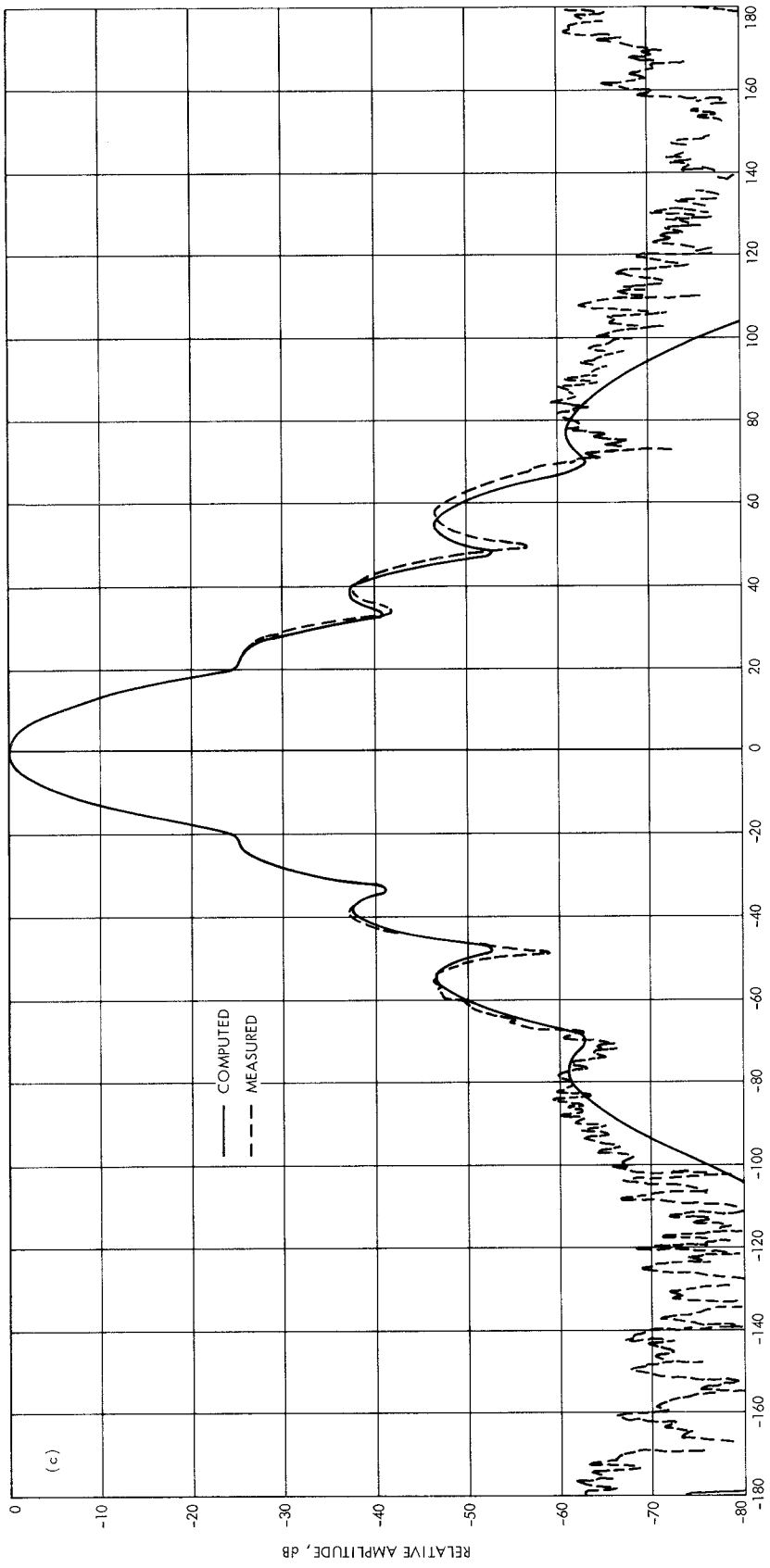
(c)
COMPUTED
MEASURED
RELATIVE AMPLITUDE, dB
0
-10
-20
-30
-40
-50
-60
-70
-80
POLAR ANGLE, deg
180
160
140
120
100
80
60
40
20
0
-20
-40
-60
-80
-100
-120
-140
-160
-180

Fig. 3 (contd)

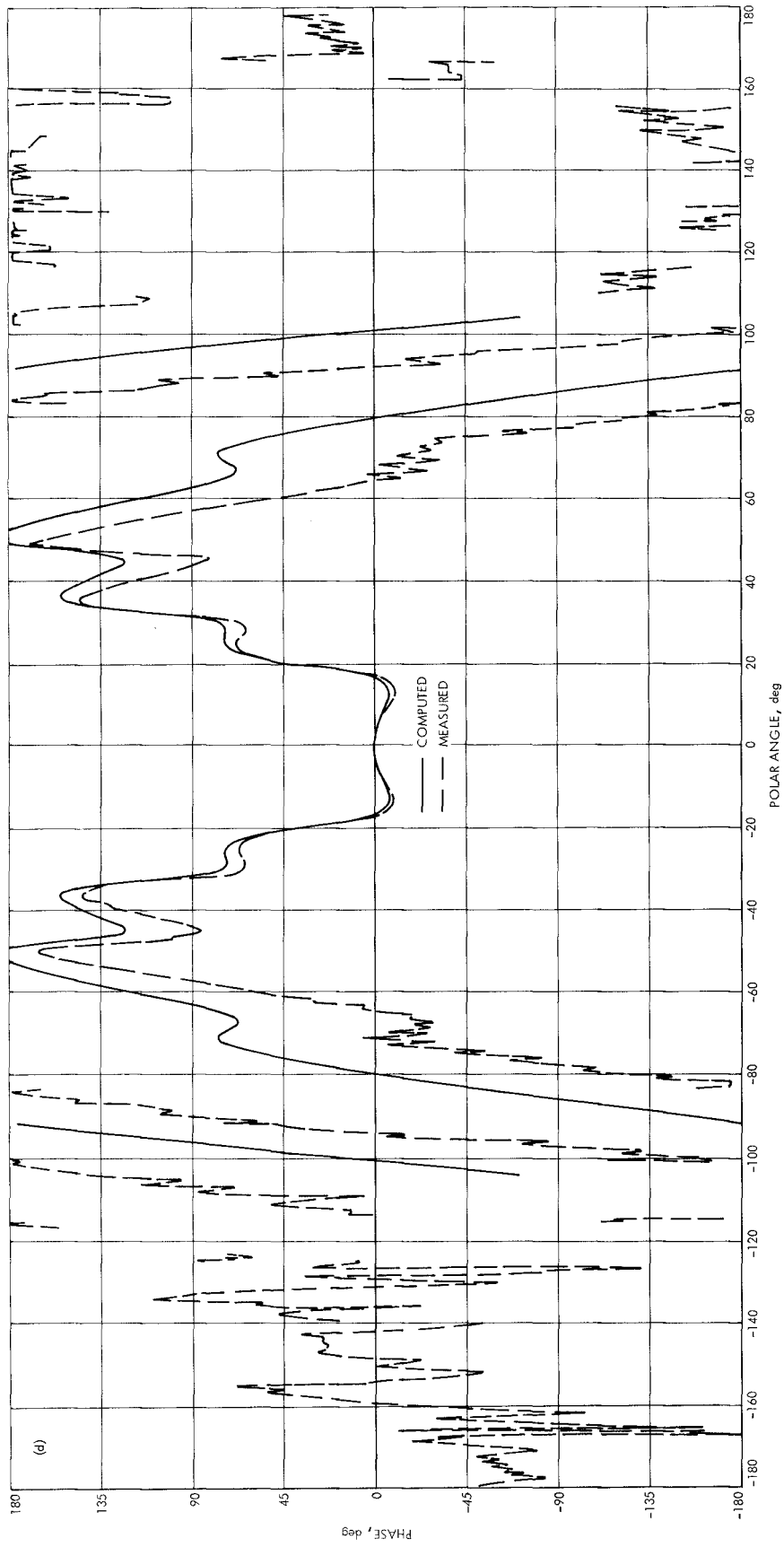
(d)
COMPUTED
MEASURED
PHASE, deg
POLAR ANGLE, deg
180
135
90
45
0
-45
-90
-135
-180
180
160
140
120
100
80
60
40
20
0
-20
-40
-60
-80
-100
-120
-140
-160
-180

Fig. 3 (contd)

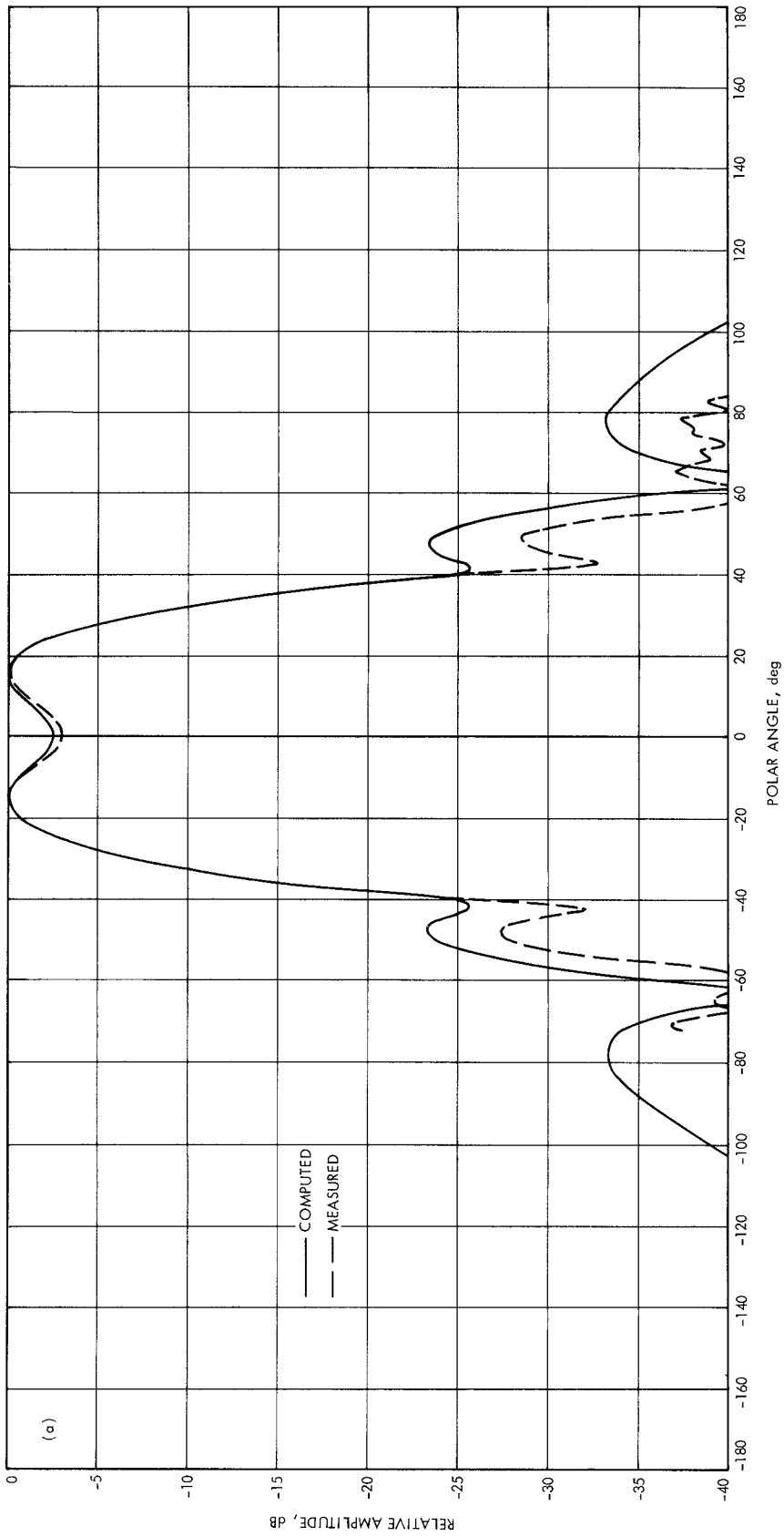

Fig. 4. Computed and measured patterns, experimental dual hybrid-mode horn: (a) E-plane amplitude, (b) H-plane amplitude

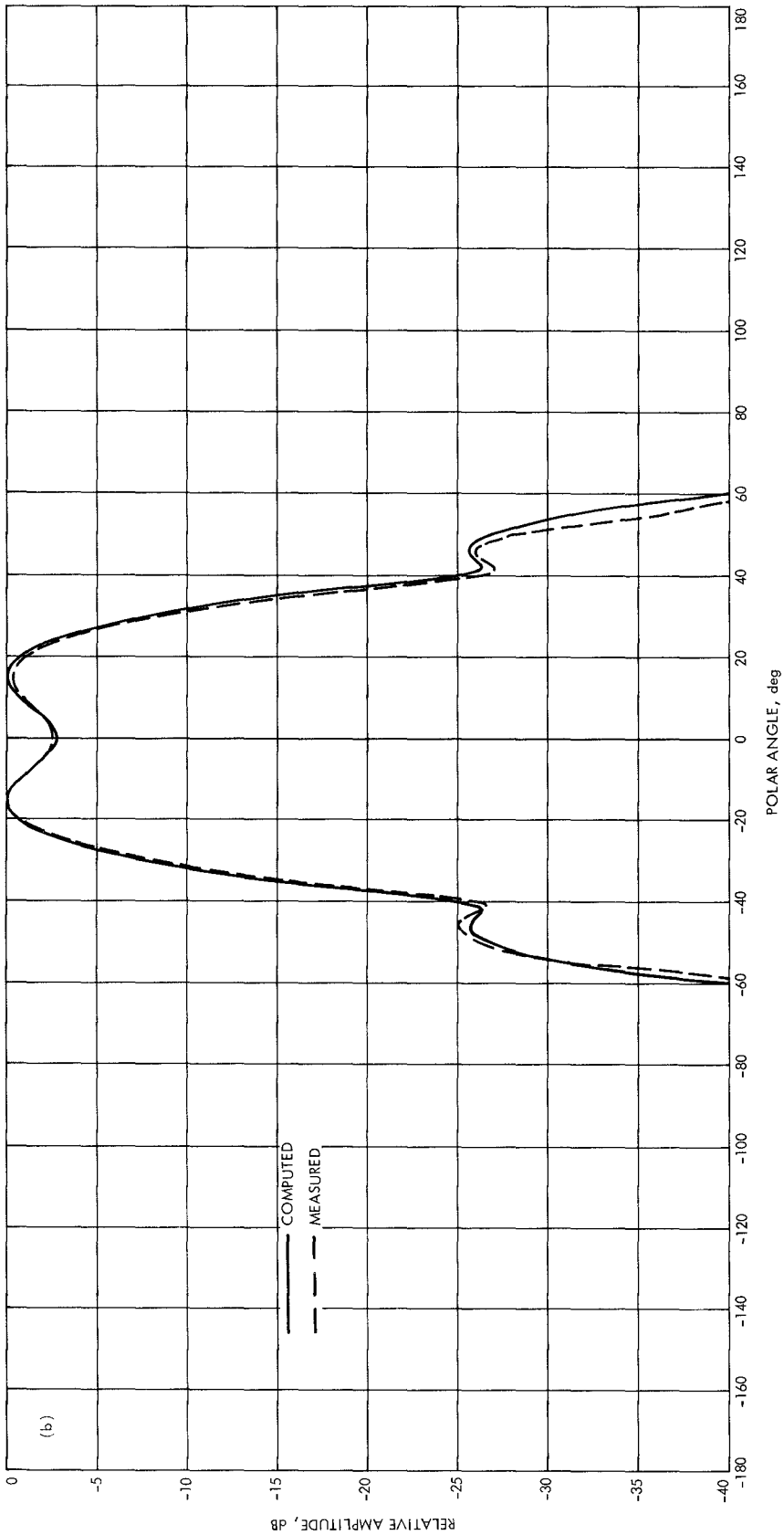
(b)
COMPUTED
MEASURED
RELATIVE AMPLITUDE, dB
0
-5
-10
-15
-20
-25
-30
-35
-40
180
160
140
120
100
80
60
40
20
0
-20
-40
-60
-80
-100
-120
-140
-160
-180
POLAR ANGLE, deg

Fig. 4 (contd)